Osmium Thioether Chemistry: Synthesis and Single-crystal X-Ray Structures of $[Os([9]aneS_3)_2][PF_6]_2 \cdot 2MeNO_2$, $[Os(4\text{-}MeC_6H_4Pr^i)([9]aneS_3)][BPh_4]_2 \cdot MeNO_2$ and $[OsH(CO)(PPh_3)([9]aneS_3)]PF_6 \cdot 0.5CH_2Cl_2$ ([9]aneS$_3$ = 1,4,7-trithiacyclononane)†

Michael N. Bell, Alexander J. Blake, Robert M. Christie, Robert O. Gould, Alan J. Holder, Timothy I. Hyde, Martin Schröder* and Lesley J. Yellowlees*
Department of Chemistry, The University of Edinburgh, West Mains Road, Edinburgh EH9 3JJ, UK

Treatment of $[\{OsCl_2(4\text{-}MeC_6H_4Pr^i)\}_2]$ with 4 molar equivalents of [9]aneS$_3$ in EtOH for 48 h followed by addition of NH_4PF_6 affords the bis(sandwich) complex $[Os([9]aneS_3)_2][PF_6]_2$ in 55% yield. An alternative and more direct route is by reaction of $[NH_4]_2[OsCl_6]$ with 2 molar equivalents of [9]aneS$_3$ in refluxing water–dimethylformamide–MeOH (3:1:1 v/v/v) for 48 h followed by addition of NH_4PF_6. The complex $[Os([9]aneS_3)_2][PF_6]_2 \cdot 2MeNO_2$ crystallises in the monoclinic space group $P2_1/a$ (alt. $P2_1/c$, no. 14) with a = 9.6621(5), b = 15.1573(8), c = 10.6367(7) Å, β = 100.524(5)° and Z = 2. A single-crystal X-ray structure determination shows a centrosymmetric cation with homoleptic thioether co-ordination at Os^{II}, Os–S(1) 2.3313(18), Os–S(4) 2.3380(19) and Os–S(7) 2.3408(20) Å, consistent with a d^6 metal centre. The ion $[Os([9]aneS_3)_2]^{2+}$ shows a reversible oxidation at $E_{\frac{1}{2}}$ = +1.16 V *vs.* ferrocene–ferrocenium. Coulometry confirms this oxidation to be a one-electron process. Electrochemical or chemical oxidation of $[Os([9]aneS_3)_2]^{2+}$ gives $[Os([9]aneS_3)_2]^{3+}$ which has been characterised by electronic and ESR spectroscopy. Reaction of $[\{OsCl_2(4\text{-}MeC_6H_4Pr^i)\}_2]$ with 2 molar equivalents of [9]aneS$_3$ in MeOH followed by addition of $NaBPh_4$ affords the mixed-sandwich complex $[Os(4\text{-}MeC_6H_4Pr^i)([9]aneS_3)][BPh_4]_2$ in 65% yield. The complex $[Os(4\text{-}MeC_6H_4Pr^i)([9]aneS_3)][BPh_4]_2 \cdot MeNO_2$ crystallises in the triclinic space group $P\bar{1}$, a = 11.5027(8), b = 13.8509(13), c = 18.3983(12) Å, α = 94.72(1), β = 105.01(3), γ = 91.28(1)° and Z = 2. The crystal structure shows facial co-ordination of both [9]aneS$_3$ and $4\text{-}MeC_6H_4Pr^i$ at octahedral Os^{II}. Interestingly, there is an unusual disorder of the trithia macrocycle with two enantiomers of [9]aneS$_3$ being present in the crystal: the two forms of the macrocycle were successfully modelled. Reaction of $[MH_2(CO)(PPh_3)_3]$ with 1 molar equivalent of [9]aneS$_3$ in the presence of NH_4PF_6 in refluxing acetone (M = Ru) or refluxing 2-methoxyethanol (M = Os) for 2 h under N_2 gives $[MH(CO)(PPh_3)([9]aneS_3)]PF_6$. The complex $[OsH(CO)(PPh_3)([9]aneS_3)]PF_6 \cdot 0.5CH_2Cl_2$ crystallises in the monoclinic space group $P2_1/n$ (alt. $P2_1/c$, no. 14) with a = 15.955(6), b = 21.929(9), c = 8.895(7) Å, β = 96.69(8)° and Z = 4. The structure shows octahedral Os^{II} with [9]aneS$_3$ bound facially, Os–S(1) 2.377(3) (*trans* to CO), Os–S(4) 2.369(3) (*trans* to PPh$_3$), Os–S(7) 2.402(3) (*trans* to H), Os–H 1.60(9), Os–P 2.3344(24) and Os–C 1.868(11) Å. The reactivity of $[MH(CO)(PPh_3)([9]aneS_3)]^+$ with O_2 and chlorinated solvents is discussed.

We have been investigating the synthesis and redox properties of complexes of [9]aneS$_3$ (1,4,7-trithiacyclononane) with third-row transition-metal ions.[1] The synthesis of macrocyclic complexes of these ions is often difficult due to the kinetic inertness of the metal ions to substitution. The trithia macrocycle [9]aneS$_3$ is preorganised for facial co-ordination to metal centres,[2] and, as a six-electron donor, is isolobal with cyclopentadienyl, arene, pyrazolylborate and tripodal triphosphine ligands. It should, therefore, form a range of organometallic half-sandwich complexes of type $[MX(Y)Z([9]aneS_3)]^{x+}$ incorporating a thioether capping ligand. We have previously reported the synthesis of $[Ir([9]aneS_3)_2]^{3+}$, $[IrCl_3([9]aneS_3)]$, $[IrH([9]aneS_3)_2]^{2+}$,[3] $[Ir([9]aneS_3)(cod)]^+$ (cod = cycloocta-1,5-diene), $[Ir([9]aneS_3)(C_2H_4)_2]^+$,[4] $[Pt([9]aneS_3)_2]^{2+}$ [5] and $[Au([9]aneS_3)_2]^{n+}$ (n = 1–3).[6] We describe herein the synthesis and structure of the homoleptic bis(sandwich) osmium(II) complex $[Os([9]aneS_3)_2]^{2+}$,[7] of the hydridocarbonyl complexes $[MH(CO)(PPh_3)([9]aneS_3)]^+$ (M = Ru or Os), and the mixed-sandwich species $[Os(4\text{-}MeC_6H_4Pr^i)([9]aneS_3)]^{2+}$. These complexes are the first reported examples of osmium complexes of [9]aneS$_3$.

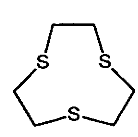
[9]aneS$_3$

† *Supplementary data available:* see Instructions for Authors, *J. Chem. Soc., Dalton Trans.*, 1992, Issue 1, pp. xx–xxv.

Results and Discussion

$[Os([9]aneS_3)_2]^{2+}$.—The synthesis of the homoleptic thioether complexes $[M([9]aneS_3)_2]^{2+}$ (M = Fe[8] or Ru[7,9]) can be achieved readily by reaction of [9]aneS$_3$ with metal(II) salts, typically $Fe(ClO_4)_2$, $[\{RuCl_2(arene)\}_2]$, $[Ru(solv)_6]^{2+}$ (solv = Me_2SO or H_2O) or from $FeCl_3$ or $RuCl_3 \cdot 3H_2O$. The preparation of the osmium(II) analogue $[Os([9]aneS_3)_2]^{2+}$, however, presents a greater challenge because of the kinetic inertness of the d^6 metal centre. Reaction of $[Os_3(CO)_{12}]$, $[OsCl_6]^{n-}$ (n = 2 or 3) salts and simple osmium(II) complexes with excess of [9]aneS$_3$ under a variety of conditions did not afford

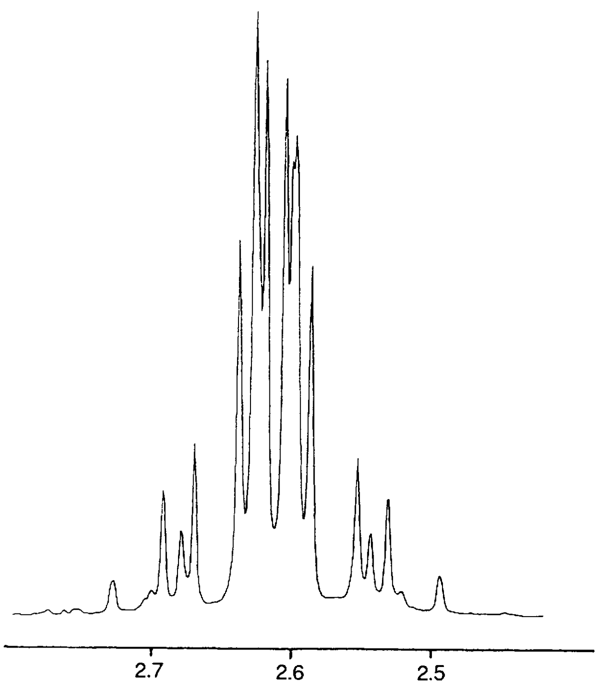

Fig. 1 Proton NMR spectrum (360 MHz, CD_3CN, 298 K) of $[Os([9]aneS_3)_2]^{2+}$

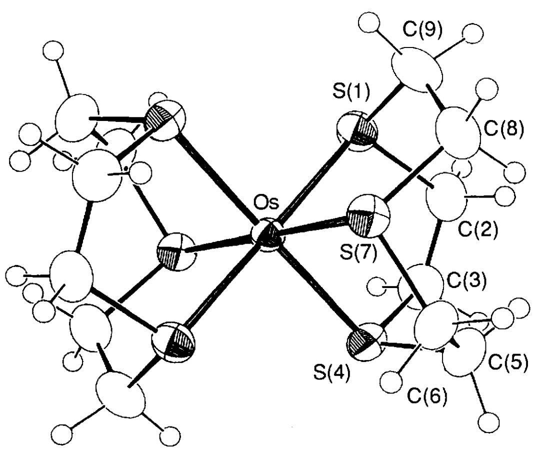

Fig. 2 Single-crystal X-ray structure of $[Os([9]aneS_3)_2]^{2+}$ with numbering scheme adopted

Table 1 Bond lengths (Å), angles and torsion angles (°) with estimated standard deviations (e.s.d.s) for $[Os([9]aneS_3)_2][PF_6]_2 \cdot 2MeCN$

Os–S(1)	2.3313(18)	C(3)–S(4)	1.848(8)
Os–S(4)	2.3380(19)	S(4)–C(5)	1.816(8)
Os–S(7)	2.3408(20)	C(5)–C(6)	1.502(11)
S(1)–C(2)	1.819(9)	C(6)–S(7)	1.823(8)
S(1)–C(9)	1.843(8)	S(7)–C(8)	1.825(8)
C(2)–C(3)	1.509(11)	C(8)–C(9)	1.532(11)
S(1)–Os–S(4)	87.92(6)	Os–S(4)–C(5)	102.1(3)
S(1)–Os–S(7)	87.87(7)	C(3)–S(4)–C(5)	101.9(4)
S(4)–Os–S(7)	87.52(7)	S(4)–C(5)–C(6)	112.9(5)
Os–S(1)–C(2)	103.3(3)	C(5)–C(6)–S(7)	112.1(5)
Os–S(1)–C(9)	106.12(25)	Os–S(7)–C(6)	105.0(3)
C(2)–S(1)–C(9)	100.7(4)	Os–S(7)–C(8)	102.4(3)
S(1)–C(2)–C(3)	113.6(6)	C(6)–S(7)–C(8)	101.7(4)
C(2)–C(3)–S(4)	112.9(5)	S(7)–C(8)–C(9)	113.6(5)
Os–S(4)–C(3)	105.13(25)	S(1)–C(9)–C(8)	111.4(5)
C(9)–S(1)–C(2)–C(3)	−67.9(6)	S(4)–C(5)–C(6)–S(7)	−50.9(7)
C(2)–S(1)–C(9)–C(8)	134.1(6)	C(5)–C(6)–S(7)–C(8)	136.2(6)
S(1)–C(2)–C(3)–S(4)	−46.6(7)	C(6)–S(7)–C(8)–C(9)	−64.7(6)
C(2)–C(3)–S(4)–C(5)	133.1(6)	S(7)–C(8)–C(9)–S(1)	−47.8(7)
C(3)–S(4)–C(5)–C(6)	−63.7(6)		

Table 2 Atomic coordinates with e.s.d.s for $[Os([9]aneS_3)_2][PF_6]_2 \cdot 2MeCN$

Atom	*x*	*y*	*z*
Os	0.5	0.5	0
S(1)	0.596 10(19)	0.573 61(12)	0.188 19(17)
C(2)	0.558 0(10)	0.500 1(4)	0.312 7(9)
C(3)	0.580 7(7)	0.403 9(5)	0.286 3(7)
S(4)	0.502 45(20)	0.371 17(12)	0.121 26(19)
C(5)	0.644 9(8)	0.309 1(5)	0.073 1(8)
C(6)	0.772 9(8)	0.364 5(5)	0.068 9(7)
S(7)	0.729 92(19)	0.465 21(14)	−0.023 56(18)
C(8)	0.834 2(7)	0.547 1(5)	0.078 2(7)
C(9)	0.788 4(7)	0.560 1(6)	0.207 4(7)
P	1.141 86(21)	0.386 63(15)	0.361 68(20)
F(1)	1.108 1(7)	0.397 5(6)	0.213 4(6)
F(2)	1.171 0(7)	0.372 9(6)	0.511 6(5)
F(3)	1.055 5(10)	0.302 1(5)	0.343 3(8)
F(4)	1.237 8(11)	0.469 4(8)	0.377 0(9)
F(5)	1.007 8(9)	0.436 8(7)	0.374 4(8)
F(6)	1.273 2(8)	0.336 6(9)	0.343 6(9)
O(1)	0.924 1(8)	0.313 1(6)	−0.180 9(7)
O(2)	0.711 2(8)	0.300 1(7)	−0.253 6(9)
N	0.824 5(9)	0.308 0(5)	−0.269 6(9)
C(1s)	0.862 3(10)	0.314 6(8)	−0.397 9(9)

$[Os([9]aneS_3)_2]^{2+}$ in workable yields. For example, reaction of $[\{OsCl_2(4\text{-}MeC_6H_4Pr^i)\}_2]$ with $[9]aneS_3$ in MeOH affords the half-sandwich complex $[Os(4\text{-}MeC_6H_4Pr^i)([9]aneS_3)]^{2+}$;[10,11] extended reflux of this complex in MeOH for 72 h, or changing to higher-boiling solvents such as ethylene glycol or dimethyl sulfoxide (dmso) gave very low yields (typically less than 5%) of the desired product $[Os([9]aneS_3)_2]^{2+}$.[11] The reaction of $[\{OsCl_2(4\text{-}MeC_6H_4Pr^i)\}_2]$ with $[9]aneS_3$ is, however, highly solvent dependent, and $[Os([9]aneS_3)_2]^{2+}$ can be prepared in up to 60% yield by reaction of these two species in EtOH for 48 h under N_2. We have also developed an alternative route which gives the product in 40% yield by direct reaction of $[NH_4]_2[OsCl_6]$ with $[9]aneS_3$ in refluxing water–dimethylformamide (dmf)–MeOH (3:1:1 v/v/v) for 48 h under N_2; $[Os([9]aneS_3)_2]^{2+}$ can be isolated as a PF_6^- or BF_4^- salt. The complex $[Os([18]aneS_6)]^{2+}$ ($[18]aneS_6$ = 1,4,7,10,13,16-hexathiacyclooctadecane) can also be prepared using this latter route by replacing $[9]aneS_3$ with $[18]aneS_6$ in the reaction.

The ^1H NMR spectrum of $[Os([9]aneS_3)_2]^{2+}$ in CD_3CN shows (Fig. 1) an ABCD pattern at δ 2.61 for the methylene protons of co-ordinated $[9]aneS_3$ as expected for an octahedral bis(sandwich) complex of type $[M[9]aneS_3)_2]^{x+}$.[7,12,13] The ^{13}C NMR spectrum shows a single resonance at δ 33.50 confirming that all the carbon centres in the complex are equivalent. Elemental analysis and IR and fast atom bombardment (FAB) mass spectroscopy further confirm the formation of $[Os([9]aneS_3)_2]^{2+}$. Single crystals of $[Os([9]aneS_3)_2][PF_6]_2 \cdot 2MeNO_2$ were grown by vapour diffusion of Et_2O into a solution of the complex in $MeNO_2$. The single-crystal X-ray structure of the complex shows (Fig. 2, Tables 1 and 2) a centrosymmetric cation with homoleptic thioether co-ordination to Os^{II}, Os–S(1) 2.3313(18), Os–S(4) 2.3380(19), Os–S(7) 2.3408(20) Å, S(1)–Os–S(4) 87.92(6), S(1)–Os–S(7) 87.87(7) and S(4)–Os–S(7) 87.52(7)°. The co-ordination is therefore very similar to that in $[Ru([9]aneS_3)_2]^{2+}$ which shows Ru–S(1) 2.3272(14), Ru–S(4) 2.3357(14), Ru–S(7) 2.3331(14) Å, S(1)–Ru–S(4) 87.87(5), S(1)–Ru–S(7) 88.09(5) and S(4)–Ru–S(7) 88.26(5)°.[7,9] FAB mass spectroscopy of $[Os([9]aneS_3)_2][PF_6]_2$ shows molecular peaks (M^+) at *m/z* 696, 550 and 522 assigned to the fragments $[^{192}Os([9]aneS_3)_2(PF_6) - H]^+$, $[^{192}Os([9]aneS_3)_2]^+$ and $[^{192}Os([9]aneS_3)_2 - C_2H_4]^+$ res-

Table 3 Redox potentials (V)* for the M^{II}–M^{III} couples of low-spin octahedral complexes $[ML_6]^{n+/(n+1)+}$

	$E_{\frac{1}{2}}$		
	Fe	Ru	Os
L = CN^- [19]	+0.12	+0.62	+0.36
L_2 = bipy [18]	+0.72	+0.92	+0.51
L_3 = terpy [18]	+0.73	+0.91	+0.60
L_3 = [9]aneS_3	+0.98	+1.41	+1.16

* Corrected for the ferrocene–ferrocenium couple in MeCN.

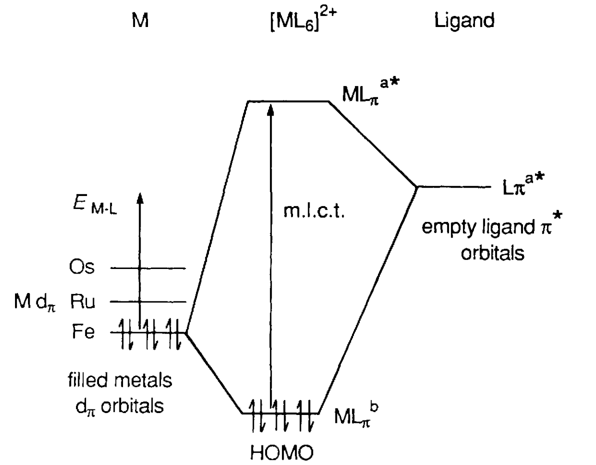

Fig. 3 Simplified molecular orbital diagram showing M–L π interactions in octahedral d^6 metal complexes; m.l.c.t. = metal to ligand charge transfer

pectively. Observation of the intense fragment at m/z 522 is significant; we observe loss of ethylene in the FAB mass spectra of many of our [9]aneS_3 complexes, and also other thioether complexes containing $-SCH_2CH_2S-$ linkages. The loss of ethylene in co-ordinated thioether complexes has been observed previously.[14] The mass spectral experiment suggests that vacuum pyrolysis of [9]aneS_3 complexes might be used synthetically for the preparation of dithiolate complexes.

The complex $[Os([9]aneS_3)_2]^{2+}$ shows an oxidation process at $E_{\frac{1}{2}}$ = +1.16 V *vs.* ferrocene–ferrocenium; this compares with values of $E_{\frac{1}{2}}$ = +1.41 and +0.98 V in MeCN for $[Ru([9]aneS_3)_2]^{2+/3+}$ (refs. 7 and 9) and low-spin $[Fe([9]aneS_3)_2]^{2+/3+}$ (refs. 8 and 15) respectively. On the basis of the relative electrode potentials it appears that the ruthenium(II) and osmium(II) centres are stabilised by homoleptic thioether co-ordination. On going from Fe to Ru to Os one might expect the 2+/3+ couple to become more cathodic reflecting the ease of oxidation of the metal centre on descending the group triad. The third ionisation potential of the free metals decreases in the order 30.7 (for Fe), 28.5 (for Ru), 25 eV (for Os) (eV ≈ 1.60×10^{-19} J).[16] The order of the 2+/3+ redox potentials for $[M([9]aneS_3)_2]^{2+/3+}$, however, follows the order Fe < Ru > Os. The same order for the 2+/3+ couples has been observed for other low-spin complexes $[M(bipy)_3]^{2+/3+}$ (bipy = 2,2′-bipyridine),[17] $[M(terpy)_2]^{2+/3+}$ (terpy = 2,2′:6′,2″-terpyridine)[18] and $[M(CN)_6]^{3-/2-}$ (ref. 19) (Table 3). The order Fe < Ru > Os therefore appears to be general for these low-spin d^6 metal complex systems and reflects the energy of the highest-occupied molecular orbital (HOMO) (Fig. 3). Overlap between the full metal-based d_π orbitals and the empty π^* orbitals of the π-accepting ligands must therefore be maximised for Ru^{II}, itself a particularly good π-donor centre. There will be a greater energy mismatch between the Fe-based d_π orbitals and the ligand π^* orbitals (E_{M-L} in Fig. 3) since the third ionisation energy for Fe is greater than for Ru. Thus, the resultant bonding molecular orbital $ML_\pi{}^b$ will have more metal character in the $[FeL_6]^{2+}$ complexes than in the analogous $[RuL_6]^{2+}$ complexes, and concomitantly the antibonding molecular orbital $ML_\pi{}^{a*}$ will have more ligand character in $[FeL_6]^{2+}$. Therefore the M^{II}–M^{III} couple is more positive for Ru than for Fe. Extension of this argument to Os suggests that the Os^{II}–Os^{III} couple would be the most positive for the three metal centres. However, the d orbitals are more diffuse on Os than on Ru and hence there will be less efficient π overlap of the osmium d_π orbitals and the π^* ligand-based orbitals than for the corresponding orbitals on Ru, with the net result that the Ru^{II}–Ru^{III} couple occurs at more positive potentials than does the Os^{II}–Os^{III} couple.

The Os^{II}–Os^{III} couple is the most cathodic of the triad for the complexes of bipy and terpy, whereas for [9]aneS_3 and CN^- the Fe^{II}–Fe^{III} couple is the most cathodic. The electrode potential of M^{II}–M^{III} for M = Fe and Os relative to one another is dependent on the poor energy and good spacial Md_π–$L_\pi{}^*$ orbital overlap for Fe *versus* the better energy match but worse spacial match of the Os system. In this sense, [9]aneS_3 is influencing the d^6 metal centre in a similar fashion to CN^- and lends further support to the postulate that the thioether donors in [9]aneS_3 really do act as overall π acceptors to d^6 metal ions such as Fe^{II}, Ru^{II} and Os^{II}. We have previously shown that the Fe–S bond lengths lengthen on oxidation of $[Fe([9]aneS_3)_2]^{2+}$ to $[Fe([9]aneS_3)_2]^{3+}$, consistent with removal of a bonding electron from $t_{2g}{}^6$ Fe^{II} to $t_{2g}{}^5$ Fe^{III}.[15] It should be noted however that the angles at the octahedral d^6 metal centres will vary appreciably on going from $[M([9]aneS_3)_2]^{x+}$ to $[M(CN)_6]^{x-}$, and this angular variation may also influence the M^{II}–M^{III} redox potentials.

Coulometry confirms the oxidation of $[Os([9]aneS_3)_2]^{2+}$ to be a one-electron process giving the intense blue product $[Os([9]aneS_3)_2]^{3+}$, the cyclic voltammogram of which is identical to that of the precursor $[Os([9]aneS_3)_2]^{2+}$. This confirms the chemical reversibility of the $[Os([9]aneS_3)_2]^{2+/3+}$ couple. The complex $[Os([9]aneS_3)_2]^{3+}$ [λ_{max} = 696, 646(sh), 514, 429 and 329 nm] decomposes over a period of 2 h in MeCN (0.1 mol dm^{-3} $NBu^n{}_4PF_6$) presumably *via* deprotonation and ring opening.[20] The stability of $[Os([9]aneS_3)_2]^{3+}$ in MeCN is greater than that of $[Ru([9]aneS_3)_2]^{3+}$ or $[Fe([9]aneS_3)_2]^{3+}$, although all three cations are stabilised by acidic media.[7,15] The X-band ESR spectrum (77 K, MeCN glass) of $[Os([9]aneS_3)_2]^{3+}$ shows $g_\perp$ = 2.358, $g_\parallel$ ≈ 1.860 (this latter component being ill defined) consistent with a metal $t_{2g}{}^5$ configuration; similar g parameters have been observed for $[Fe([9]aneS_3)_2]^{3+}$ and $[Ru([9]aneS_3)_2]^{3+}$.[7] The complex $[Os([9]aneS_3)_2]^{3+}$ can also be generated by oxidation of $[Os([9]aneS_3)_2]^{2+}$ with $NOBF_4$ in H_2SO_4 or $HClO_4$. The relative instability of the 3+ cations is clearly a result of the stabilisation of d^6 metal(II) species by homoleptic thioether co-ordination. This can be ascribed to the relatively weak σ-donor ability of thioether ligands,[21] and to their significant π-acceptor ability.[15] The π-acceptor abilities of thioether S-donors [whether *via* acceptor d orbitals or *via* σ*(S–C) antibonding orbitals[22]] are probably maximised with strong π-donor $t_{2g}{}^6$ metal ions such as Ru^{II}.

Half-sandwich Osmium(II) *Complexes*.—As part of a study of half-sandwich complexes of [9]aneS_3 with the platinum-group metals we have investigated the synthesis of half-sandwich osmium(II) complexes. Our work on mixed-sandwich complexes $[Ru(arene)([9]aneN_3)]^{2+}$ demonstrated[10,11] that it was possible to isolate these species only for systems incorporating a strong metal–arene bond. With [9]aneS_3 the complex $[Ru([9]aneS_3)_2]^{2+}$ was invariably isolated although the intermediacy of species $[Ru(arene)([9]aneS_3)]^{2+}$ was clear. Since third-row transition metals in general, and Os^{II} in particular, are known to form stronger bonds with arenes than their second-row analogues, it seemed likely that mixed arene–[9]aneS_3 complexes could be isolated with Os^{II}.

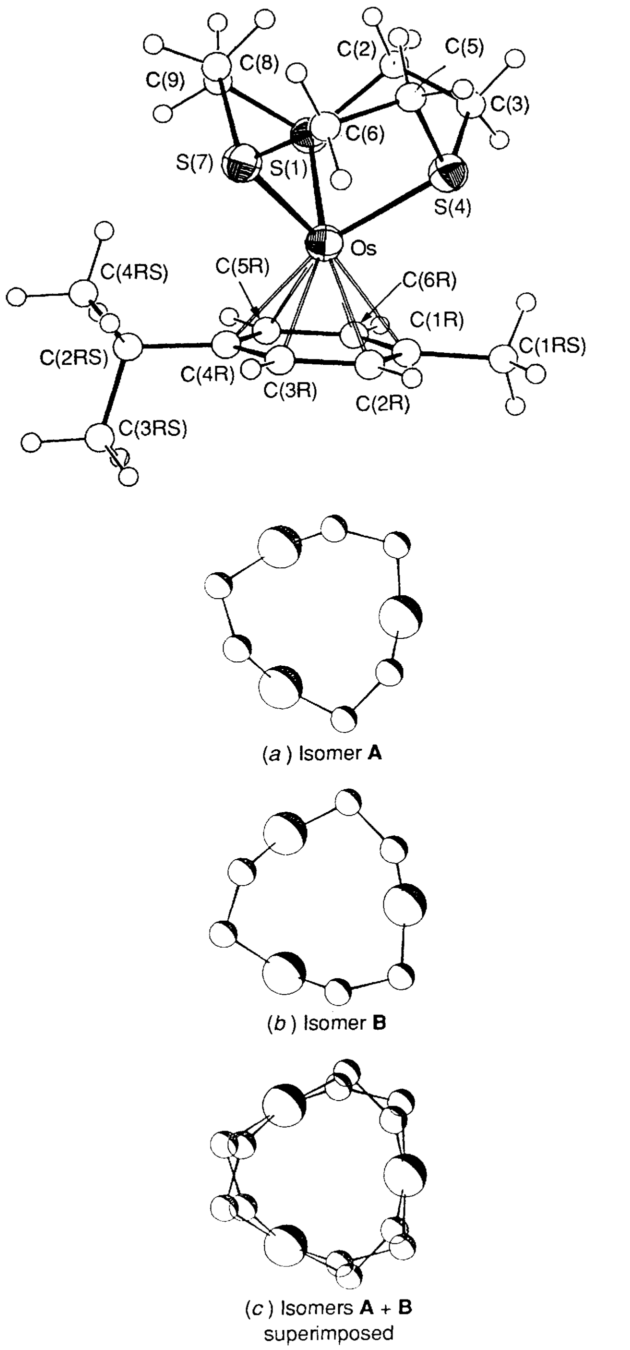

Fig. 4 Single-crystal X-ray structure of the major enantiomer of $[Os(4\text{-}MeC_6H_4Pr^i)([9]aneS_3)]^{2+}$ with numbering scheme adopted; (*a*)–(*c*) show the enantiomers of co-ordinated [9]aneS_3

$[Os(4\text{-}MeC_6H_4Pr^i)([9]aneS_3)]^{2+}$. The complex $[\{OsCl_2(4\text{-}MeC_6H_4Pr^i)\}_2]$ was treated with 2 mole equivalents of [9]aneS_3 in gently refluxing MeOH. Over a period of an hour the yellow colour of the osmium dimer faded to leave a colourless solution. Addition of excess of $NaBPh_4$ afforded a white solid which was recrystallised from a $MeNO_2$–Et_2O to yield colourless crystals. The IR and ^1H NMR spectra of the product confirmed the presence of [9]aneS_3 [δ_H 2.76 (s, br)], 4-$MeC_6H_4Pr^i$ [δ_H 1.20 (d, Me), 2.35 (spt), 6.39, 6.55 (A_2B_2)] and BPh_4^- in a 1:1:2 ratio. A resonance at δ_H 4.41 was attributed to the presence of $MeNO_2$ in the crystals. Elemental analysis confirmed the formulation as the mixed-sandwich complex $[Os(4\text{-}MeC_6H_4Pr^i)([9]aneS_3)][BPh_4]_2\cdot MeNO_2$. Single crystals were obtained from $MeNO_2$–Et_2O and an X-ray structural

Table 4 Bond lengths (Å), angles and torsion angles (°) of the idealised enantiomers of [9]aneS_3 in $[Os(4\text{-}MeC_6H_4Pr^i)([9]aneS_3)]^{2+}$

S(1)–C(2)	1.8480	1.8233
S(1)–C(9)	1.8233	1.8480
C(2)–C(3)	1.5124	1.5124
C(3)–S(4)	1.8233	1.8480
S(4)–C(5)	1.8480	1.8233
C(5)–C(6)	1.5124	1.5124
C(6)–S(7)	1.8233	1.8480
S(7)–C(8)	1.8480	1.8233
C(8)–C(9)	1.5124	1.5124
C(2)–S(1)–C(9)	101.357	101.357
S(1)–C(2)–C(3)	111.741	114.258
C(2)–C(3)–S(4)	114.258	111.741
C(3)–S(4)–C(5)	101.357	101.357
S(4)–C(5)–C(6)	111.741	114.258
C(5)–C(6)–S(7)	114.258	111.741
C(6)–S(7)–C(8)	101.357	101.357
S(7)–C(8)–C(9)	111.741	114.258
S(1)–C(9)–C(8)	114.258	111.741
C(9)–S(1)–C(2)–C(3)	133.508	66.507
C(2)–S(1)–C(9)–C(8)	−66.507	−133.508
S(1)–C(2)–C(3)–S(4)	−47.092	47.092
C(2)–C(3)–S(4)–C(5)	−66.507	−133.508
C(3)–S(4)–C(5)–C(6)	133.508	66.507
S(4)–C(5)–C(6)–S(7)	−47.092	47.092
C(5)–C(6)–S(7)–C(8)	−66.507	−133.508
C(6)–S(7)–C(8)–C(9)	133.508	66.507
S(7)–C(8)–C(9)–S(1)	−47.092	47.092

determination undertaken. The overall geometry of the mixed-sandwich cation is as predicted (Fig. 4), with one face of the octahedral osmium(II) centre co-ordinated by 4-$MeC_6H_4Pr^i$ and the opposite face by [9]aneS_3. The macrocycle shows an unusual disorder. Both enantiomers **A** and **B** of [9]aneS_3 present in each cation are twisted by 60° with respect to one another; Fig. 4(*c*) shows these superimposed upon one another.

Following the approach used successfully to model disorder present in the structure of $[Rh([9]aneS_3)_2]^{3+}$,[13] an idealised macrocycle was generated and fitted onto the existing sulfur co-ordinates. There were still three main peaks in the difference map all approximately 2.3 Å distant from the osmium centre, suggesting alternative sulfur positions. To model this twist of the macrocycle ideal groups were fitted onto the two sets of sulfur co-ordinates. The major isomer present in the cation was refined as enantiomer **A**. To establish which enantiomer was present in the minor site, both ideal groups were transposed onto the new sulfur positions and the occupancies allowed to refine. After several cycles of least squares the occupancy of **B** had refined to 0.25, where as enantiomer **A** had disappeared (occupancy 0.01) and was deleted. The two idealised macrocycles, the major isomer, enantiomer **A**, and the minor isomer, enantiomer **B**, were then allowed to refine as rigid groups, absorbing the unassigned electron density in the difference map and leaving no peak above 0.59 e $Å^{-3}$. The occupancies of the two sites refined to 0.72 and 0.28 respectively. Owing to the distinct asymmetry imparted by the side groups on the ring, the *p*-cymene will effectively fix the position of the cation within the crystal. Both positions of the cation and trithia macrocycle give a staggered configuration at Os relative to three C–C bonds in the *p*-cymene. The bond distances, angles and torsion angles for the two idealised enantiomers are listed in Table 4. The bond distances and angles are very similar and it is only when comparing the respective torsion angles that the differences between the two enantiomers becomes obvious. Bond lengths, angles, torsion angles and atomic coordinates for $[Os(4\text{-}MeC_6H_4Pr^i)([9]aneS_3)][BPh_4]_2\cdot MeNO_2$ are given in Tables 5 and 6.

Although the complex $[Os(4\text{-}MeC_6H_4Pr^i)([9]aneS_3)]^{2+}$ could be converted into $[Os([9]aneS_3)_2]^{2+}$ by extended

Table 5 Bond lengths (Å), angles and torsion angles (°) with e.s.d.s for $[Os(4\text{-}MeC_6H_4Pr^i)([9]aneS_3)][BPh_4]_2\cdot MeNO_2$

Os–S(1)	2.3207(14)	Os–C(6R)	2.234(5)
Os–S(4)	2.3594(14)	C(1R)–C(2R)	1.397(7)
Os–S(7)	2.3439(14)	C(1R)–C(6R)	1.417(7)
Os–S(1′)	2.281(5)	C(1R)–C(1RS)	1.507(8)
Os–S(4′)	2.442(5)	C(2R)–C(3R)	1.425(7)
Os–S(7′)	2.375(5)	C(3R)–C(4R)	1.423(7)
Os–C(1R)	2.281(5)	C(4R)–C(5R)	1.424(7)
Os–C(2R)	2.239(5)	C(4R)–C(2RS)	1.505(8)
Os–C(3R)	2.223(5)	C(5R)–C(6R)	1.396(7)
Os–C(4R)	2.275(5)	C(2RS)–C(3RS)	1.534(11)
Os–C(5R)	2.223(5)	C(2RS)–C(4RS)	1.486(10)
S(1)–Os–S(4)	87.64(5)	Os–S(7′)–C(6′)	107.2(3)
S(1)–Os–S(7)	88.02(5)	Os–S(7′)–C(8′)	101.8(3)
S(4)–Os–S(7)	87.12(5)	C(2R)–C(1R)–C(6R)	117.9(5)
S(1′)–Os–S(4′)	86.60(18)	C(2R)–C(1R)–C(1RS)	121.1(5)
S(1′)–Os–S(7′)	88.20(18)	C(6R)–C(1R)–C(1RS)	121.0(5)
S(4′)–Os–S(7′)	84.55(18)	C(1R)–C(2R)–C(3R)	121.0(4)
Os–S(1)–C(2)	106.58(8)	C(2R)–C(3R)–C(4R)	121.3(4)
Os–S(1)–C(9)	102.42(7)	C(3R)–C(4R)–C(5R)	116.5(4)
Os–S(4)–C(3)	101.99(7)	C(3R)–C(4R)–C(2RS)	123.9(5)
Os–S(4)–C(5)	106.13(8)	C(5R)–C(4R)–C(2RS)	119.5(5)
Os–S(7)–C(6)	103.07(7)	C(4R)–C(5R)–C(6R)	121.6(5)
Os–S(7)–C(8)	105.60(8)	C(1R)–C(6R)–C(5R)	121.6(5)
Os–S(1′)–C(2′)	106.2(3)	C(4R)–C(2RS)–C(3RS)	107.9(5)
Os–S(1′)–C(9′)	105.7(3)	C(4R)–C(2RS)–C(4RS)	115.0(6)
Os–S(4′)–C(3′)	103.3(3)	C(3RS)–C(2RS)–C(4RS)	111.6(6)
Os–S(4′)–C(5′)	105.2(3)		

C(6R)–C(1R)–C(2R)–C(3R)	−1.7(7)
C(1RS)–C(1R)–C(2R)–C(3R)	179.0(5)
C(2R)–C(1R)–C(6R)–C(5R)	1.6(8)
C(1RS)–C(1R)–C(6R)–C(5R)	−179.0(5)
C(1R)–C(2R)–C(3R)–C(4R)	−0.7(7)
C(2R)–C(3R)–C(4R)–C(5R)	3.1(7)
C(2R)–C(3R)–C(4R)–C(2RS)	−175.1(5)
C(3R)–C(4R)–C(5R)–C(6R)	−3.2(7)
C(2RS)–C(4R)–C(5R)–C(6R)	175.1(5)
C(3R)–C(4R)–C(2RS)–C(3RS)	93.5(7)
C(3R)–C(4R)–C(2RS)–C(4RS)	−31.9(8)
C(5R)–C(4R)–C(2RS)–C(3RS)	−84.7(6)
C(5R)–C(4R)–C(2RS)–C(4RS)	150.0(6)
C(4R)–C(5R)–C(6R)–C(1R)	0.9(8)

reaction with $[9]aneS_3$, this species is not particularly useful for the preparation of complexes of type $[OsX(Y)Z([9]aneS_3)]^{x+}$. We wished to develop synthetic routes to relatively labile half-sandwich complexes of $[9]aneS_3$ with Os^{II} and this led to synthetic routes to $[OsCl_2(PPh_3)([9]aneS_3)]$ and $[MH(CO)(PPh_3)([9]aneS_3)]^+$ (M = Ru or Os).

$[OsCl_2(PPh_3)([9]aneS_3)]$. Reaction of $[OsCl_2(PPh_3)_3]$ with $[9]aneS_3$ in CH_2Cl_2 at 273 K for 4 d gave a green solution. Addition of Et_2O afforded a green product, the IR spectrum of which confirms the presence of PPh_3 and $[9]aneS_3$. The FAB mass spectrum of the product shows molecular ion peaks (M^+) at *m/z* 704 and 669 assigned to $[^{192}Os^{35}Cl_2(PPh_3)([9]aneS_3)]^+$ and $[^{192}Os^{35}Cl(PPh_3)([9]aneS_3)]^+$ respectively. A peak at *m/z* 931 assigned to $[^{192}Os^{35}Cl(PPh_3)_2([9]aneS_3)]^+$ is also observed suggesting that this species might be isolable; interestingly, our initial attempts to prepare $[RuCl(PPh_3)_2([9]aneS_3)]^+$ have been unsuccessful.[23,24] The complex $[OsCl_2(PPh_3)([9]aneS_3)]$ shows a reversible Os^{II}–Os^{III} couple at $E_{\frac{1}{2}} = +0.0305$ V *vs.* ferrocene–ferrocenium: this compares with a value of $E_{\frac{1}{2}} = +0.30$ V for $[RuCl_2(PPh_3)([9]aneS_3)]$.[23]

$[MH(CO)(PPh_3)([9]aneS_3)]^+$ (M = Ru or Os). Reaction of $[RuH_2(CO)(PPh_3)_3]$ with 1 molar equivalent of $[9]aneS_3$ in refluxing CH_2Cl_2 for 15 h under N_2 afforded a light yellow solution. On removal of solvent, addition of EtOH and NH_4PF_6 afforded a yellow precipitate. The ^{31}P NMR spectrum of this product showed one singlet resonance at δ 30.83, while the ^1H NMR spectrum showed no resonance attributable to a metal hydride but confirmed the presence of $[9]aneS_3$ and PPh_3 in a 1 : 1 ratio. The IR and FAB mass spectra and analytical data confirmed the isolated complex to be $[RuCl(CO)(PPh_3)([9]aneS_3)]PF_6$; this same complex could also be prepared by reaction of $[RuCl_2(CO)(PPh_3)(dmf)]$ with $[9]aneS_3$ in ethanol, or by reaction of $[RuCl_2(PPh_3)([9]aneS_3)]$ with $TlPF_6$ in CH_2Cl_2 in the presence of CO. The target hydrido-complex $[RuH(CO)(PPh_3)([9]aneS_3)]PF_6$ was successfully prepared by reaction of $[RuH_2(CO)(PPh_3)_3]$ with $[9]aneS_3$ in refluxing acetone. It is colourless and oxygen-sensitive in solution. The complex shows a ν(CO) stretching vibration at 1982s(br) cm^{-1} with a weaker and sharper band at 1910 cm^{-1} tentatively assigned to a ν(Ru–H) stretching vibration. The FAB mass spectrum shows a peak at *m/z* 573 assigned to $[^{102}RuH(CO)(PPh_3)([9]aneS_3)]^+$ while the ^1H NMR spectrum in $(CD_3)_2CO$ under N_2 shows a doublet resonance at δ −9.29 (J_{HP} = 20.8 Hz), and confirms the 1:1 ratio of $[9]aneS_3$ to PPh_3. The ^{31}P NMR spectrum shows a single, doublet resonance at δ 48.19; selective decoupling experiments confirm coupling between the co-ordinated hydride and PPh_3. The complex is not stable in oxygenated solvents. Dissolution of the colourless $[RuH(CO)(PPh_3)([9]aneS_3)]^+$ in acetone at 293 K under air leads within minutes to the development of a greenish tinge to the solution. This colouration deepens over 1 h and then fades to give a yellow solution from which a yellow precipitate can be isolated. This precipitate appears to contain at least two as yet unknown P-containing products, the ^{31}P NMR spectrum showing two resonances at δ 38.10 and 30.56.

In CH_2Cl_2 under air, $[RuH(CO)(PPh_3)([9]aneS_3)]^+$ decomposes *via* a green-blue solution to afford after 48 h at 293 K a yellow solution from which the yellow complex $[RuCl(CO)(PPh_3)([9]aneS_3)]^+$ can be isolated. Thus, abstraction of Cl^- from CH_2Cl_2 appears to have occurred with the conversion of a monohydrido complex into the corresponding chloro-species; importantly, this result suggests that the $Ru(CO)(PPh_3)([9]aneS_3)$ fragment is maintained in the blue-green intermediates observed in the reactions of $[RuH(CO)(PPh_3)([9]aneS_3)]^+$ in oxygenated solvents, and that oxidation of the co-ordinated thioether appears not to be occurring under these conditions. It is tempting to postulate superoxy and hydroxy complexes such as $[Ru(OOH)(CO)(PPh_3)([9]aneS_3)]^{2+}$ and $[Ru(OH)(CO)(PPh_3)([9]aneS_3)]^{2+}$ and carbonyl-bridged binuclear species such as $[([9]aneS_3)(Ph_3P)Ru(CO)_2Ru(PPh_3)([9]aneS_3)]^{4+}$ as intermediates in the above reactions. Solutions of the blue-green intermediate show a weak ESR signal similar to those observed in the reactions of ruthenium(II) porphyrins with O_2.[25] This ESR signal, and an absorption band at 15 960 cm^{-1} in the electronic spectrum, are each clearly associated with the intermediate green-blue species.

Unlike its ruthenium analogue, $[OsH_2(CO)(PPh_3)_3]$ does not react with 1 molar equivalent of $[9]aneS_3$ in refluxing acetone. However, if the reaction is carried out in refluxing 2-methoxyethanol for 2 h under N_2, $[OsH(CO)(PPh_3)([9]aneS_3)]PF_6$ can be isolated in 79% yield. The FAB mass spectrum of the complex shows molecular peaks at *m/z* 663 and 606 assigned to $[^{192}OsH(CO)(PPh_3)([9]aneS_3)]^+$ and $[^{192}Os(PPh_3)(SC_2H_4SC_2H_4S)]^+$ respectively. The IR spectrum shows a strong, broad band at 1967 cm^{-1} assigned to the CO stretching vibration, ν(CO), and a weaker, sharper band at 2000 cm^{-1} assigned to the Os–H stretching vibration, ν(Os–H). The ^1H NMR spectrum shows a doublet resonance at δ −10.2 (J_{PH} = 18.0 Hz) assigned to a metal hydride species, together with resonances at δ 2.41–3.52 (12 H) and 7.48–7.78 (15 H) assigned to co-ordinated $[9]aneS_3$ and PPh_3 respectively. The ^{31}P NMR spectrum shows a single doublet resonance at δ 13.19. The formulation $[OsH(CO)(PPh_3)([9]aneS_3)]PF_6$ was confirmed by elemental analysis.

Colourless crystals of $[OsH(CO)(PPh_3)([9]aneS_3)]PF_6\cdot 0.5CH_2Cl_2$ suitable for a diffraction study were grown by slow

Table 6 Atomic coordinates with e.s.d.s for $[Os(4\text{-}MeC_6H_4Pr^i)([9]aneS_3)][BPh_4]_2\cdot MeNO_2$

Atom	*x*	*y*	*z*	Atom	*x*	*y*	*z*
Os	0.400 620(10)	0.302 500(10)	0.227 830(10)	C(141)	0.601 80(19)	0.217 700(21)	−0.025 69(16)
S(1)	0.347 21(13)	0.322 33(10)	0.099 56(7)	C(142)	0.544 14(19)	0.258 84(21)	−0.091 18(16)
C(2)	0.273 74(13)	0.439 07(10)	0.089 01(7)	C(143)	0.425 78(19)	0.229 41(21)	−0.129 39(16)
C(3)	0.317 43(13)	0.508 30(10)	0.159 43(7)	C(144)	0.365 09(19)	0.158 17(21)	−0.102 10(16)
S(4)	0.319 66(13)	0.454 52(10)	0.247 38(7)	C(145)	0.422 75(19)	0.116 32(21)	−0.036 60(16)
C(5)	0.157 61(13)	0.430 29(10)	0.236 44(7)	C(146)	0.541 10(19)	0.145 74(21)	0.001 60(16)
C(6)	0.132 20(13)	0.329 38(10)	0.255 96(7)	B(2)	0.285 4(5)	0.249 9(4)	0.532 8(3)
S(7)	0.206 69(13)	0.233 92(10)	0.212 54(7)	C(211)	0.268 5(3)	0.154 99(18)	0.466 77(16)
C(8)	0.129 48(13)	0.237 33(10)	0.111 73(7)	C(212)	0.342 8(3)	0.076 84(18)	0.481 64(16)
C(9)	0.217 88(13)	0.236 30(10)	0.063 50(7)	C(213)	0.325 6(3)	−0.004 59(18)	0.429 47(16)
S(1′)	0.211 3(5)	0.309 8(4)	0.244 7(3)	C(214)	0.234 1(3)	−0.007 88(18)	0.362 46(16)
S(4′)	0.304 9(5)	0.229 8(4)	0.100 2(3)	C(215)	0.159 8(3)	0.070 28(18)	0.347 60(16)
S(7′)	0.370 0(5)	0.451 9(4)	0.172 4(3)	C(216)	0.177 0(3)	0.151 72(18)	0.399 75(16)
C(1R)	0.579 3(4)	0.362 2(4)	0.306 9(3)	C(221)	0.245 0(3)	0.352 10(18)	0.489 66(19)
C(2R)	0.600 2(4)	0.311 5(4)	0.243 0(3)	C(222)	0.332 7(3)	0.416 66(18)	0.479 07(19)
C(3R)	0.556 6(4)	0.213 6(4)	0.221 0(3)	C(223)	0.298 8(3)	0.500 78(18)	0.443 73(19)
C(4R)	0.491 6(4)	0.163 6(3)	0.263 7(3)	C(224)	0.177 2(3)	0.520 34(18)	0.418 98(19)
C(5R)	0.467 4(4)	0.218 0(4)	0.326 8(3)	C(225)	0.089 4(3)	0.455 77(18)	0.429 57(19)
C(6R)	0.510 6(4)	0.313 9(4)	0.347 9(3)	C(226)	0.123 4(3)	0.371 65(18)	0.464 92(19)
C(1RS)	0.627 0(6)	0.465 3(4)	0.331 0(3)	C(231)	0.429 59(21)	0.260 60(23)	0.585 22(16)
C(2RS)	0.451 6(6)	0.058 1(4)	0.247 0(4)	C(232)	0.522 43(21)	0.254 71(23)	0.549 25(16)
C(3RS)	0.548 8(8)	−0.000 7(5)	0.295 4(5)	C(233)	0.642 23(21)	0.262 41(23)	0.591 95(16)
C(4RS)	0.422 0(8)	0.021 3(4)	0.165 8(5)	C(234)	0.669 16(21)	0.276 00(23)	0.670 60(16)
B(1)	0.743 0(5)	0.256 2(4)	0.022 0(3)	C(235)	0.576 31(21)	0.281 90(23)	0.706 57(16)
C(111)	0.735 45(25)	0.358 60(17)	0.078 17(16)	C(236)	0.456 54(21)	0.274 19(23)	0.663 87(16)
C(112)	0.636 26(25)	0.416 61(17)	0.060 17(16)	C(241)	0.196 9(3)	0.227 98(22)	0.590 30(18)
C(113)	0.635 66(25)	0.504 70(17)	0.102 63(16)	C(242)	0.180 6(3)	0.132 78(22)	0.606 55(18)
C(114)	0.734 21(25)	0.534 80(17)	0.163 10(16)	C(243)	0.111 6(3)	0.112 88(22)	0.656 19(18)
C(115)	0.833 39(25)	0.476 79(17)	0.181 12(16)	C(244)	0.059 0(3)	0.188 15(22)	0.689 55(18)
C(116)	0.834 01(25)	0.388 69(17)	0.138 65(16)	C(245)	0.075 3(3)	0.283 34(22)	0.673 30(18)
C(121)	0.823 83(24)	0.283 42(20)	−0.039 01(15)	C(246)	0.144 3(3)	0.303 25(22)	0.623 67(18)
C(122)	0.908 80(24)	0.360 98(20)	−0.021 68(15)	C	0.896 2(7)	0.139 8(6)	0.478 1(5)
C(123)	0.983 44(24)	0.375 44(20)	−0.069 08(15)	N	0.827 6(6)	0.194 1(8)	0.419 9(5)
C(124)	0.973 11(24)	0.312 34(20)	−0.133 78(15)	O(1)	0.827 8(9)	0.179 0(10)	0.359 0(5)
C(125)	0.888 12(24)	0.234 79(20)	−0.151 11(15)	O(2)	0.774 6(11)	0.254 0(12)	0.435 1(6)
C(126)	0.813 50(24)	0.220 34(20)	−0.103 71(15)	C(2′)	0.119 1(5)	0.224 0(4)	0.174 7(3)
C(131)	0.809 7(3)	0.166 32(19)	0.072 65(16)	C(3′)	0.140 3(5)	0.225 2(4)	0.097 1(3)
C(132)	0.857 0(3)	0.090 46(19)	0.036 29(16)	C(5′)	0.312 9(5)	0.322 6(4)	0.039 8(3)
C(133)	0.908 5(3)	0.014 01(19)	0.076 34(16)	C(6′)	0.288 3(5)	0.422 7(4)	0.070 1(3)
C(134)	0.912 7(3)	0.013 39(19)	0.152 76(16)	C(8′)	0.253 7(5)	0.500 5(4)	0.210 3(3)
C(135)	0.865 4(3)	0.089 26(19)	0.189 12(16)	C(9′)	0.153 3(5)	0.427 9(4)	0.209 9(3)
C(136)	0.813 9(3)	0.165 72(19)	0.149 05(16)				

vapour diffusion of Et_2O into a solution of the complex in CH_2Cl_2. The single-crystal X-ray structure of the complex shows (Fig. 5) octahedral Os^{II} with $[9]aneS_3$ bound facially, Os–S(1) 2.377(3) (*trans* to CO), Os–S(4) 2.369(3) (*trans* to PPh_3), Os–S(7) 2.402(3) (*trans* to H), Os–H 1.60(9), Os–P 2.3344(24), Os–C 1.868(11) Å, S(1)–Os–S(4) 85.85(9), S(1)–Os–S(7) 85.97(9) and S(4)–Os–S(7) 86.45(9)°. Bond lengths, angles, torsion angles, and atomic co-ordinates are given in Tables 7 and 8. The crystallographic data described herein show that the Os–S(thioether) bond length is clearly related to the ligand *trans* to it, the Os–S bond length increasing in the order arene, $SR_2 < PPh_3 < CO < H^-$.

The complex $[OsH(CO)(PPh_3)([9]aneS_3)]^+$ is relatively stable in oxygenated solvents with only a faint green colouration observed after 2 weeks in solution at 293 K. This contrasts with the observed reactions of $[RuH(CO)(PPh_3)([9]aneS_3)]^+$ in oxygenated solvents. Interestingly, photolysis of the related dihydridoosmium(II) species $[OsH_2(CO)(C_6Me_6)]$ leads to insertion into the C–H bonds of hydrocarbons RH to give products $[OsR(H)(CO)(C_6Me_6)]$.[26] Current work aims to synthesise and study the reactivity of further examples of electrophilic, organometallic complexes of Ru^{II} and Os^{II} with thioether crowns.

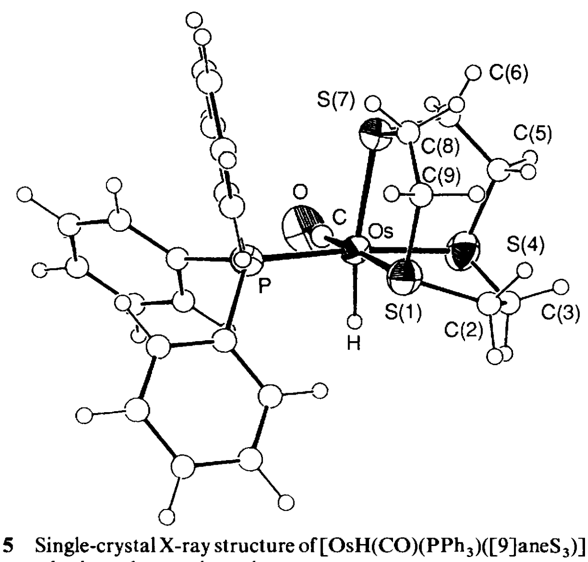

Fig. 5 Single-crystal X-ray structure of $[OsH(CO)(PPh_3)([9]aneS_3)]^+$ with numbering scheme adopted

Experimental

Infrared spectra were measured as Nujol mulls, KBr and CsI discs using a Perkin Elmer 598 spectrometer over the range 200–4000 cm^{-1}, UV/VIS spectra in quartz cells using Perkin Elmer Lambda 9 and Philips Analytical SP8-400 spectrophotometers. Microanalyses were performed by the Edinburgh

Table 7 Bond lengths (Å), angles and torsion angles (°) with e.s.d.s for $[OsH(CO)(PPh_3)([9]aneS_3)]PF_6 \cdot 0.5CH_2Cl_2$

Os–H	1.60(9)	Os–P	2.3344(24)	C(3)–S(4)	1.824(13)	C(8)–C(9)	1.393(19)
Os–C	1.868(11)	C–O	1.149(14)	S(4)–C(5)	1.823(14)	P–C(11)	1.814(7)
Os–S(1)	2.377(3)	S(1)–C(2)	1.776(14)	C(5)–C(6)	1.490(18)	P–C(21)	1.825(6)
Os–S(4)	2.369(3)	S(1)–C(9)	1.803(14)	C(6)–S(7)	1.815(12)	P–C(31)	1.823(7)
Os–S(7)	2.402(3)	C(2)–C(3)	1.434(19)	S(7)–C(8)	1.794(13)		
H–Os–C	76(3)	S(1)–Os–P	89.90(9)	Os–S(4)–C(5)	106.3(4)	Os–P–C(31)	117.50(23)
H–Os–S(1)	99(3)	S(4)–Os–S(7)	86.45(9)	C(3)–S(4)–C(5)	101.3(6)	C(11)–P–C(21)	105.3(3)
H–Os–S(4)	81(3)	S(4)–Os–P	173.65(9)	S(4)–C(5)–C(6)	114.4(9)	C(11)–P–C(31)	98.5(3)
H–Os–S(7)	166(3)	S(7)–Os–P	97.97(9)	C(5)–C(6)–S(7)	116.1(9)	C(21)–P–C(31)	104.6(3)
H–Os–P	95(3)	Os–C–O	177.1(10)	Os–S(7)–C(6)	103.3(4)	P–C(11)–C(12)	116.5(5)
C–Os–S(1)	175.1(3)	Os–S(1)–C(2)	105.8(4)	Os–S(7)–C(8)	105.7(4)	P–C(11)–C(16)	123.4(5)
C–Os–S(4)	91.5(3)	Os–S(1)–C(9)	105.5(5)	C(6)–S(7)–C(8)	101.4(6)	P–C(21)–C(22)	120.4(5)
C–Os–S(7)	98.1(3)	C(2)–S(1)–C(9)	100.8(6)	S(7)–C(8)–C(9)	120.6(10)	P–C(21)–C(26)	119.2(5)
C–Os–P	92.4(3)	S(1)–C(2)–C(3)	119.1(10)	S(1)–C(9)–C(8)	121.9(10)	P–C(31)–C(32)	118.2(5)
S(1)–Os–S(4)	85.85(9)	C(2)–C(3)–S(4)	119.0(10)	Os–P–C(11)	116.82(23)	P–C(31)–C(36)	121.7(5)
S(1)–Os–S(7)	85.97(9)	Os–S(4)–C(3)	102.4(4)	Os–P–C(21)	112.31(22)		
C(9)–S(1)–C(2)–C(3)	−109.1(11)	C(6)–S(7)–C(8)–C(9)	−103.1(11)	C(11)–P–C(21)–C(26)	133.0(5)	C(13)–C(12)–C(11)–P	176.6(5)
C(2)–S(1)–C(9)–C(8)	105.8(12)	S(7)–C(8)–C(9)–S(1)	−0.2(16)	C(31)–P–C(21)–C(22)	−157.2(5)	C(15)–C(16)–C(11)–P	−176.4(5)
S(1)–C(2)–C(3)–S(4)	20.9(15)	C(21)–P–C(11)–C(12)	176.2(5)	C(31)–P–C(21)–C(26)	29.6(6)	C(23)–C(22)–C(21)–P	−173.1(5)
C(2)–C(3)–S(4)–C(5)	79.2(11)	C(21)–P–C(11)–C(16)	−7.3(6)	C(11)–P–C(31)–C(32)	−58.2(6)	C(25)–C(26)–C(21)–P	173.2(5)
C(3)–S(4)–C(5)–C(6)	−132.1(10)	C(31)–P–C(11)–C(12)	−76.0(5)	C(11)–P–C(31)–C(36)	119.5(6)	C(33)–C(32)–C(31)–P	177.8(5)
S(4)–C(5)–C(6)–S(7)	42.6(12)	C(31)–P–C(11)–C(16)	100.5(6)	C(21)–P–C(31)–C(32)	50.2(6)	C(35)–C(36)–C(31)–P	−177.7(5)
C(5)–C(6)–S(7)–C(8)	72.9(10)	C(11)–P–C(21)–C(22)	−53.9(6)	C(21)–P–C(31)–C(36)	−132.1(5)		

University Chemistry Department microanalytical service. The ESR spectra were recorded as solids or as frozen glasses down to 77 K using a Bruker ER200D X-band spectrometer. Electrochemical measurements were performed on a Bruker E310 Universal Modular Polarograph. All readings were taken using a three-electrode potentiostatic system in acetonitrile containing 0.1 mol dm^{-3} $NBu^n{}_4PF_6$ or $NBu^n{}_4BF_4$ as supporting electrolyte. Cyclic voltammetric measurements were carried out using a double platinum electrode and a Ag–AgCl reference electrode. All potentials are quoted *versus* ferrocene–ferrocenium. Mass spectra were run by electron impact on a Kratos MS 902 and by fast atom bombardment (FAB) (3-nitrobenzyl alcohol matrix) on a Kratos MS 50TC spectrometer. Proton, ^{13}C and ^{31}P NMR spectra were recorded at 80.13, 50.32 and 36.23 MHz respectively on Bruker WP80, WP200 and JEOL FX90 spectrometers. Additionally, ^1H NMR spectra were recorded at 360 MHz on a Bruker WH360 spectrometer.

Synthesis of $[Os([9]aneS_3)_2][PF_6]_2 \cdot MeNO_2$.—The complex $[\{OsCl_2(4\text{-}MeC_6H_4Pr^i)\}_2]$ (30 mg, 0.038 mmol) was refluxed in dry methanol with $[9]aneS_3$ (28 mg, 0.15 mmol) for 72 h. Excess of NH_4PF_6 was added to the resulting mixture and the solvent removed *in vacuo*. The residue was taken up in $MeNO_2$ and addition of Et_2O to this solution afforded the complex as a light brown solid which was dried *in vacuo*. Yield = 11 mg, 31% (Found: C, 17.6; H, 2.95; N, 1.45. Calc. for $C_{13}H_{27}F_{12}NO_2OsP_2S_6$: C, 17.30; H, 3.00; N, 1.55%). IR (KBr disc): 2930 and 1423 cm^{-1}. ^1H NMR $[(CD_3)_2SO$, 80 MHz, 298 K]: δ 2.67 (br, s, 12 H, CH_2).

Synthesis of $[Os([9]aneS_3)_2][PF_6]_2$.—(*i*) The complex $[\{OsCl_2(4\text{-}MeC_6H_4Pr^i)\}_2]$ (63.6 mg, 0.08 mmol) and $[9]aneS_3$ (28.8 mg, 0.16 mmol) were refluxed together in EtOH for 48 h to afford a dark brown solution. On addition of NH_4PF_6 in water a brown product precipitated. This was collected and recrystallised from the minimum volume of hot water and dried *in vacuo*. Yield: 71.5 mg, 55%.

(*ii*) The salt $[NH_4]_2[OsCl_6]$ (100 mg, 2.28 mmol) and $[9]aneS_3$ (100 mg, 5.56 mmol) were refluxed for 48 h in a solvent mix of water (15 cm^3), dmf (5 cm^3) and MeOH (5 cm^3) under N_2. The resulting solution was taken to dryness and MeCN (20 cm^3) added. The hot solution was filtered to remove a dark brown impurity, and excess of NH_4PF_6 in water added. Solvent was removed *in vacuo* until crystallisation of the product occurred. The crude crystalline product, which may contain a purple impurity, was collected and recrystallised from MeCN and Et_2O to afford $[Os([9]aneS_3)_2][PF_6]_2$ as white crystals. Replacement of NH_4PF_6 with $NaBF_4$ affords the corresponding BF_4^- salt.

$[Os([9]aneS_3)_2][PF_6]_2$ (Found: C, 17.2; H, 2.85. Calc. for $C_{12}H_{24}F_{12}OsP_2S_6$: C, 17.15; H, 2.90%): FAB mass spectrum *m/z* 696 {calc. 696, $[^{192}Os([9]aneS_3)_2(PF_6) - H]^+$}, 550 {550, $[^{192}Os([9]aneS_3)_2]^+$} and 522 {522, $[^{192}Os([9]aneS_3)_2 - C_2H_4]^+$}; NMR ($CD_3CN$, 295 K), ^1H (360 MHz) δ 2.61 (ABCD, 12 H, CH_2); ^{13}C (50.32 MHz), δ 33.50 (CH_2); IR (KBr disc) 2950m, 1448m, 1412m, 1296w, 1266w, 1169w, 1135m, 1124w, 1084m, 1066w, 1032w, 1014w, 940w, 840vs, 742m, 709w, 676w, 659w, 558s, 464w and 320w cm^{-1}.

$[Os([9]aneS_3)_2][BF_4]_2$ (Found: C, 19.60; H, 3.45. Calc. for $C_{12}H_{24}B_2F_8OsS_6$: C, 19.85; H, 3.35%); FAB mass spectrum: *m/z* 638 {calc. 638, $[^{192}Os([9]aneS_3)_2(BF_4) - H]^+$}, 550 {550, $[^{192}Os([9]aneS_3)_2]^+$} and 522 {522, $[^{192}Os([9]aneS_3)_2 - C_2H_4]^+$}.

X-Ray Structure Determination of $[Os([9]aneS_3)_2][PF_6]_2 \cdot 2MeNO_2$.—A colourless plate (0.42 × 0.42 × 0.12 mm) suitable for X-ray analysis was obtained by vapour diffusion of Et_2O into a solution of the complex in $MeNO_2$.

Crystal data. $C_{14}H_{30}F_{12}N_2O_4OsP_2S_6$, M = 962.75, monoclinic, space group $P2_1/a$ (alt. $P2_1/c$, no. 14), a = 9.6621(5), b = 15.1573(8), c = 10.6367(7) Å, β = 100.524(5)°, U = 1531.6 Å^3 [from 2θ values of 48 reflections measured at ±ω (2θ = 30–32°, λ = 0.710 73 Å)], Z = 2 (implying that each cation lies on a crystallographic inversion centre), D_c = 2.087 g cm^{-3}, T = 298 K, μ = 4.762 mm^{-1}, $F(000)$ = 940.

Data collection and processing. Stoë STADI-4 four-circle diffractometer, graphite-monochromated Mo-Kα X-radiation, T = 298 K, ω–2θ scans with ω scan width (0.90 + 0.347 tanθ)°, 2118 unique data ($2\theta_{max}$ 45°, h −10 to 10, k 0–16, l 0–11), semiempirical absorption correction applied (minimum and maximum transmission factors 0.1042 and 0.3410 respectively), giving 1715 with $F \geqslant 6\sigma(F)$ for use in all calculations. No significant crystal decay or movement was observed.

Structure solution and refinement. From an osmium position inferred from cell contents and intensity statistics, iterative cycles of least-squares refinement and Fourier difference syn-

Table 8 Atomic coordinates with e.s.d.s for $[OsH(CO)(PPh_3)([9]aneS_3)]PF_6{\cdot}0.5CH_2Cl_2$

Atom	*x*	*y*	*z*	Atom	*x*	*y*	*z*
Os	0.428 850(20)	0.641 590(20)	0.428 94(4)	C(12)	0.546 2(4)	0.751 6(3)	0.717 4(7)
H	0.521 8(26)	0.619(5)	0.490(11)	C(13)	0.570 5(4)	0.778 3(3)	0.858 0(7)
C	0.429 3(6)	0.640 5(5)	0.639 0(12)	C(14)	0.537 1(4)	0.834 6(3)	0.893 3(7)
O	0.430 7(5)	0.637 3(4)	0.768 2(9)	C(15)	0.479 3(4)	0.864 1(3)	0.787 9(7)
S(1)	0.437 98(16)	0.636 77(13)	0.164 4(3)	C(16)	0.455 1(4)	0.837 4(3)	0.647 3(7)
S(4)	0.404 22(18)	0.535 11(13)	0.413 5(3)	C(21)	0.384 0(4)	0.791 4(3)	0.324 9(6)
S(7)	0.279 55(16)	0.653 33(12)	0.361 2(3)	C(22)	0.309 7(4)	0.804 7(3)	0.387 1(6)
P	0.465 69(15)	0.744 61(12)	0.428 86(23)	C(23)	0.243 9(4)	0.834 9(3)	0.300 6(6)
P(2)	0.728 59(21)	0.535 52(16)	0.187 8(4)	C(24)	0.252 3(4)	0.851 8(3)	0.151 9(6)
F(1)	0.691 1(6)	0.568 6(4)	0.319 1(11)	C(25)	0.326 5(4)	0.838 6(3)	0.089 7(6)
F(2)	0.803 8(6)	0.510 4(5)	0.296 4(11)	C(26)	0.392 4(4)	0.808 4(3)	0.176 2(6)
F(3)	0.675 3(6)	0.477 6(4)	0.219 6(12)	C(31)	0.562 2(4)	0.765 0(3)	0.349 7(8)
F(4)	0.653 7(6)	0.559 1(5)	0.075 6(11)	C(32)	0.582 0(4)	0.826 7(3)	0.338 8(8)
F(5)	0.761 8(6)	0.499 8(5)	0.055 5(11)	C(33)	0.656 8(4)	0.844 1(3)	0.283 7(8)
F(6)	0.780 7(6)	0.592 7(4)	0.160 7(12)	C(34)	0.711 8(4)	0.799 9(3)	0.239 6(8)
C(2)	0.449 0(9)	0.558 2(6)	0.122 1(14)	C(35)	0.692 0(4)	0.738 2(3)	0.250 5(8)
C(3)	0.449 7(8)	0.514 4(6)	0.241 7(14)	C(36)	0.617 2(4)	0.720 7(3)	0.305 5(8)
C(5)	0.291 9(8)	0.525 6(6)	0.352 6(15)	Cl(3)	0.054 1(15)	0.503 9(11)	0.036(3)
C(6)	0.238 4(7)	0.577 7(5)	0.391 4(13)	Cl(1)	0.076 8(9)	0.472 8(6)	0.161 3(17)
C(8)	0.264 6(8)	0.658 4(6)	0.158 5(13)	Cl(2)	0.034 2(12)	0.487 9(9)	0.434 3(24)
C(9)	0.332 6(8)	0.651 2(7)	0.074 9(16)	C(2S)	0.047 9(24)	0.467 6(17)	0.292(5)
C(11)	0.488 5(4)	0.781 1(3)	0.612 0(7)	Cl(4)	0.003(4)	0.484 3(24)	0.114(7)

thesis located all non-H atoms. At isotropic convergence, final corrections (minimum 0.877, maximum 1.212) for absorption effects were made using DIFABS.[27] Non-H atoms were then refined (by least squares on F^2[28]) with anisotropic thermal parameters: macrocyclic H atoms were included at fixed, calculated positions and solvent H atoms refined as part of a rigid group. At final convergence R, R' = 0.0401, 0.0582 respectively, S = 1.221 for 191 refined parameters and the final ΔF synthesis showed no peak above 1.04 e Å^{-3}. The weighting scheme $w^{-1} = \sigma^2(F) + 0.001\,93F^2$ gave satisfactory agreement analyses, a secondary extinction parameter refined to 6.1(19) × 10^{-8} and in the final cycle $(\Delta/\sigma)_{max}$ was 0.036.

Synthesis of $[Os(4\text{-}MeC_6H_4Pr^i)([9]aneS_3)][BPh_4]_2{\cdot}MeNO_2$.—The complex $[\{OsCl_2(4\text{-}MeC_6H_4Pr^i)\}_2]$ (30 mg, 0.038 mmol) was allowed to react with [9]aneS_3 (14 mg, 0.076 mmol) in refluxing MeOH (20 cm^3) under N_2 for 1 h. Addition of $NaBPh_4$ to the cooled solution afforded a cream precipitate which was recrystallised from $MeNO_2$–Et_2O to give colourless crystals. Yield = 25 mg, 65% (Found: C, 64.3; H, 5.65; N, 1.40. Calc. for $C_{65}H_{69}B_2NO_2OsS_3$: C, 64.70; H, 5.75; N, 1.15%). IR (KBr disc): 2930, 1430, 1554 and 1373 cm^{-1}. ^{1}H NMR [$(CD_3)_2SO$, 80 MHz, 298 K]: δ 1.20 (d, 6 H, CH*Me*$_2$), 2.35 (spt, *C*HMe$_2$, 1 H), 2.76 (br s, CH_2, 12 H), 6.39 and 6.55 (A_2B_2, CH, 4 H).

Crystal Structure Determination of $[Os(4\text{-}MeC_6H_4Pr^i)([9]aneS_3)][BPh_4]_2{\cdot}MeNO_2$.—A colourless plate (0.5 × 0.54 × 0.23 mm) suitable for X-ray analysis was obtained by vapour diffusion of Et_2O into a solution of the complex in $MeNO_2$.

Crystal data. $C_{65}H_{69}B_2NO_2OsS_3$, M = 1204.27, triclinic, space group $P\bar{1}$, a = 11.5027(8), b = 13.8509(13), c = 18.3983(12) Å, α = 94.72(1), β = 105.01(3), γ = 91.28(1)°, U = 2818 Å^3 (by least-squares refinement on diffractometer angles for 14 centred reflections), $\bar{\lambda}$ = 0.710 73 Å), Z = 2, D_c = 1.418 g cm^{-3}, T = 298 K, μ(Mo-Kα) = 2.385 mm^{-1}.

Data collection and processing. STADI-4 diffractometer, ω–2θ mode with ω scan width (0.8 + 0.347 tanθ)°, graphite monochromated Mo-Kα radiation; 7375 reflections measured, ($2\theta_{max}$ 45°, h −12 to 12, k −14 to 14, l 0–19) giving 6404 with $F \geqslant 2\sigma(F)$. Initial absorption correction applied (minimum and maximum transmission factors 0.1345 and 0.2371). A correction for slight crystal decay was applied during data reduction.

Structure analysis and refinement. A Patterson synthesis located the Os and subsequent iterative cycles of least-squares refinement and Fourier difference syntheses revealed the positions of all non-hydrogen atoms.[28] Both enantiomeric forms of [9]aneS_3 were present and these were refined as idealised rigid groups with the site occupancies summing to one. At isotropic convergence empirical corrections for absorption were applied, (DIFABS;[27] minimum and maximum corrections 0.905 and 1.072). Full-matrix least squares with H atoms in calculated positions and anisotropic thermal motion for all fully occupied non-H atoms. The weighting scheme $w^{-1} = \sigma^2(F) + 0.000\,106F^2$ gave satisfactory agreement analyses. Final R and R' were 0.0292 and 0.0379 for 583 parameters refined and the final ΔF synthesis showed maximum peak and minimum trough of 0.59 and −0.87 e Å^{-3}.

Synthesis of $[OsCl_2(PPh_3)([9]aneS_3)]$.—The complex $[OsCl_2(PPh_3)_3]$ (125 mg, 0.119 mmol) was stirred with [9]aneS_3 (25 mg, 0.139 mmol) in CH_2Cl_2 (40 cm^3) under N_2 for 96 h at 298 K to give a green solution. The solvent volume was reduced to 15 cm^3 and addition of Et_2O afforded a green precipitate which was collected and dried *in vacuo*. Yield = 58 mg, 70% (Found: C, 40.80; H, 4.00. Calc. for $C_{24}H_{27}Cl_2OsPS_3$: C, 40.90; H, 3.85%). FAB mass spectrum: m/z 704 {calc. 704, $[^{192}Os^{35}Cl_2(PPh_3)([9]aneS_3)]^+$} and 669 {669, $[^{192}Os^{35}Cl(PPh_3)([9]aneS_3)]^+$}.

Synthesis of $[RuCl(CO)(PPh_3)([9]aneS_3)]PF_6$.—(*i*) Reaction of $[RuCl_2(CO)(PPh_3)(dmf)]$ (106.6 mg, 0.134 mmol) with [9]aneS_3 (24.1 mg, 0.134 mmol) in refluxing EtOH for 10 min afforded a pale yellow solution. Addition of excess of NH_4PF_6 in water gave a yellow precipitate which was collected, washed with EtOH (1 cm^3) and Et_2O and dried *in vacuo*. Yield = 82.4 mg, 82%.

(*ii*) Reaction of $[RuH_2(CO)(PPh_3)_3]$ (107.4 mg, 0.117 mmol) and [9]aneS_3 (21.1 mg, 0.117 mmol) in refluxing CH_2Cl_2 under N_2 for 15 h afforded a yellow solution. The solvent was removed under reduced pressure and the residue redissolved in a small amount of hot EtOH (8 cm^3). Addition of excess of NH_4PF_6 in water gave a yellow precipitate which was collected, washed with EtOH (1 cm^3) and Et_2O, and dried *in vacuo*. Yield = 72.8 mg, 83% (Found: C, 39.6; H, 3.50. Calc. for $C_{25}H_{27}ClF_{12}OP_2S_3$: C, 39.90; H, 3.60%). IR: 2010 cm^{-1} [ν(CO)]. FAB mass spectrum: m/z 607 {calc. 607, $[^{102}Ru^{35}Cl(CO)(PPh_3)([9]aneS_3)]^+$}, 573 {572, $[^{102}Ru(CO)(PPh_3)([9]aneS_3)]^+$}, 551 {551, $[^{102}Ru^{35}Cl(PPh_3)([9]aneS_3) - C_2H_4]^+$} and 516 {516, $[^{102}Ru(PPh_3)([9]aneS_3) - C_2H_4]^+$}. NMR $[(CD_3)_2CO$, 295 K]: ^{31}P (36.23 MHz), δ 30.83; ^1H (80 MHz), δ 2.08–3.57 (m, CH_2, 12 H) and 7.38–7.81 (m, CH, 15 H).

Synthesis of $[RuH(CO)(PPh_3)([9]aneS_3)]PF_6$.—Reaction of $[RuH_2(CO)(PPh_3)_3]$ (113.0 mg, 0.123 mmol) and [9]aneS_3 (22.1 mg, 0.123 mmol) in the presence of NH_4PF_6 in refluxing acetone under N_2 for 2 h afforded a colourless solution. Degassed EtOH (8 cm^3) was added and the solution held at reflux for 2 h. The solvent was removed under reduced pressure until a white precipitate formed, and the mixture cooled to 0 °C. The white product was collected, recrystallised from degassed CH_2Cl_2-hexane and dried *in vacuo*. Yield = 69.8 mg, 79% (Found: C, 40.7; H, 3.85. Calc. for $C_{25}H_{28}F_{12}OP_2RuS_3 \cdot 0.5CH_2Cl_2$: C, 40.3; H, 3.85%). IR: 1982 [ν(CO)] and 1910 cm^{-1} [ν(Ru–H)]. FAB mass spectrum; *m/z* 573 {calc. 573, $[^{102}RuH(CO)(PPh_3)([9]aneS_3)]^+$} and 516 {516, $[^{102}Ru(PPh_3)([9]aneS_3) - C_2H_4]^+$}. NMR $[(CD_3)_2CO$, 295 K]: ^{31}P (36.23 MHz), δ 48.19 (d, J_{HP} = 20.9); ^1H (80 MHz), δ − 9.30 (d, Ru–H, J_{HP} = 20.9 Hz), 2.38–3.38 (m, CH_2, 12 H) and 7.47–7.80 (m, CH, 15 H).

Synthesis of $[OsH(CO)(PPh_3)([9]aneS_3)]PF_6$.—The complex $[OsH_2(CO)(PPh_3)_3]$ (129.5 mg, 0.129 mmol), [9]aneS_3 (23.2 mg, 0.129 mmol) and excess of NH_4PF_6 were heated under reflux in 2-methoxyethanol (8 cm^3) under N_2 for 2 h. On reducing the volume of the solution to 4 cm^3 and adding Et_2O a light brown precipitate was formed. This was collected and recrystallised from $MeNO_2$–Et_2O to give a white product which was dried *in vacuo*. Yield = 82.0 mg, 79% (Found: C, 37.0; H, 3.50. Calc. for $C_{25}H_{28}F_6OOsP_2S_3$: C, 37.15; H, 3.50%). IR: 1967 [ν(CO)] and 2000 cm^{-1} [ν(Os–H)]. FAB mass spectrum: *m/z* 663 {calc. 663, $[^{192}OsH(CO)(PPh_3)([9]aneS_3)]^+$} and 606 {606, $[^{192}Os(PPh_3)([9]aneS_3) - C_2H_4]^+$}. NMR $[(CD_3)_2CO$, 295 K]: ^{31}P (36.23 MHz), δ 13.19 (d, J_{PH} = 18.0); ^1H (80 MHz), δ −10.20 (d, Ru–H, J_{HP} = 18.0 Hz), 2.41–3.52 (m, CH_2, 12 H) and 7.48–7.78 (m, CH, 15 H).

X-Ray Structure Determination of $[OsH(CO)(PPh_3)([9]aneS_3)]PF_6 \cdot 0.5CH_2Cl_2$.—A colourless lath (1.00 × 0.40 × 0.12 mm) suitable for X-ray analysis was obtained by vapour diffusion of Et_2O into a solution of the complex in CH_2Cl_2.

Crystal data. $C_{25}H_{28}F_6OOsP_2S_3 \cdot 0.5CH_2Cl_2$, *M* = 849.3, monoclinic, space group $P2_1/n$ (alt. $P2_1/c$, no. 14), *a* = 15.955(6), *b* = 21.929(9), *c* = 8.895(7) Å, β = 96.69(8)°, *U* = 3091 Å^3 (from setting angles for 13 reflections with 2θ = 14–24°, $\bar{\lambda}$ = 0.710 73 Å), *Z* = 4, D_c = 1.825 g cm^{-3}, *T* = 298 K, μ = 4.570 mm^{-1}, *F*(000) = 1660.

Data collection and processing. Stoë STADI-2 two-circle diffractometer, graphite-monochromated Mo-Kα X-radiation, *T* = 298 K, ω scans with width [1.50 + 0.75 (sinμ/tanθ)]°, 5871 reflections measured ($2\theta_{max}$ 50°, *h* −18 to 18, *k* 0–26, *l* 0–10), giving 3760 with $F \geq 6\sigma(F)$ for use in all calculations. No significant crystal decay or movement was observed.

Structure solution and refinement. The osmium position was derived from a Patterson synthesis and subsequent iterative cycles of least-squares refinement and Fourier difference synthesis located all non-H atoms.[28] At isotropic convergence, corrections for absorption effects were applied using DIFABS.[27] The structure was then refined (by least squares on *F*), with phenyl rings as idealised hexagons and with H atoms included at fixed, calculated positions, apart from the hydride which was constrained to be 1.60 Å from the Os. At final convergence *R*, *R′* = 0.0527, 0.0562 respectively, *S* = 1.161 for 210 refined parameters and the final Δ*F* synthesis showed no peak above 1.33 e Å^{-3}. The weighting scheme $w^{-1} = \sigma^2(F) + 0.000\,242F^2$ gave satisfactory agreement analyses and in the final cycle $(\Delta/\sigma)_{max}$ was 0.01.

Atomic scattering factors were inlaid,[28] or taken from ref. 29. Molecular geometry calculations utilised CALC[30] and the Figures were produced by ORTEP II.[31]

Additional material available from the Cambridge Crystallographic Data Centre comprises H-atom coordinates, thermal parameters and remaining bond lengths and angles.

Acknowledgements

We thank the Royal Society of Edinburgh and Scottish Office Education Department for a Support Research Fellowship (to M. S.), the University of Edinburgh for support (to M. N. B.), the SERC for support, and Johnson Matthey plc for generous loans of platinum metal salts.

References

1 A. J. Blake and M. Schroder, *Adv. Inorg. Chem.*, 1990, **35**, 1; M. N. Bell, A. J. Blake, R. O. Gould, A. J. Holder, T. I. Hyde, A. J. Lavery, G. Reid and M. Schröder, *J. Inclusion Phenom.*, 1987, **5**, 169.
2 R. S. Glass, G. S. Wilson and W. N. Setzer, *J. Am. Chem. Soc.*, 1980, **102**, 5068; see also, R. D. Hancock and A. E. Martell, *Comments Inorg. Chem.*, 1988, **6**, 237; R. Blom, D. W. H. Rankin, H. E. Robertson, M. Schroder and A. Taylor, *J. Chem. Soc., Perkin Trans 2*, 1991, 773.
3 A. J. Blake, R. O. Gould, A. J. Holder, T. I. Hyde, G. Reid and M. Schröder, *J. Chem. Soc., Dalton Trans.*, 1990, 1759.
4 A. J. Blake, M. A. Halcrow and M. Schröder, *J. Chem. Soc., Chem. Commun.*, 1991, 253.
5 A. J. Blake, R. O. Gould, A. J. Holder, T. I. Hyde, M. O. Odulate, A. J. Lavery and M. Schroder, *J. Chem. Soc., Chem. Commun.*, 1987, 118.
6 A. J. Blake, R. O. Gould, J. A. Greig, A. J. Holder, T. I. Hyde and M. Schröder, *J. Chem. Soc., Chem. Commun.*, 1989, 876; A. J. Blake, J. A. Greig, A. J. Holder, T. I. Hyde, A. Taylor and M. Schröder, *Angew Chem.*, 1990, **102**, 203; *Angew Chem., Int. Ed. Engl.*, 1990, **29**, 197.
7 M. N. Bell, A. J. Blake, H.-J. Kuppers, M. Schröder and K. Wieghardt, *Angew. Chem.*, 1987, **99**, 253; *Angew. Chem., Int. Ed. Engl.*, 1987, **26**, 250; M. N. Bell, A. J. Blake, A. J. Holder, T. I. Hyde and M. Schröder, *J. Chem. Soc., Dalton Trans.*, 1990, 3841.
8 H.-J. Kuppers, K. Wieghardt, B. Nuber, J. Weiss, E. Bill and A. X. Trautwein, *Inorg. Chem.*, 1987, **26**, 3762.
9 S. C. Rawle and S. R. Cooper, *J. Chem. Soc., Chem. Commun.*, 1987, 308; S. C. Rawle, T. J. Sewell and S. R. Cooper, *Inorg. Chem.*, 1987, **22**, 3769.
10 M. N. Bell, Ph.D. Thesis, University of Edinburgh, 1987.
11 M. Schröder, *Pure Appl. Chem.*, 1988, **60**, 517.
12 K. Wieghardt, H.-J. Kuppers and J. Weiss, *Inorg. Chem.*, 1985, **24**, 3067; H.-J. Küppers, A. Neves, C. Pomp, D. Ventur, K. Wieghardt, B. Nuber and J. Weiss, *Inorg. Chem.*, 1986, **25**, 2400; G. S. Wilson, D. D. Swanson and R. S. Glass, *Inorg. Chem.*, 1986, **25**, 3827.
13 A. J. Blake, R. O. Gould, A. J. Holder, T. I. Hyde and M. Schröder, *J. Chem. Soc., Dalton Trans.*, 1988, 1861.
14 S. J. Ibrahim and C. J. Pickett, *J. Chem. Soc., Chem. Commun.*, 1991, 246; see also, D. L. Dubois, W. K. Miller and M. Rakowski-Dubois, *J. Am. Chem. Soc.*, 1981, **103**, 3429; D. Sellmann, I. Barth, F. Knoch and M. Moll, *Inorg. Chem.*, 1990, **29**, 1822.
15 A. J. Blake, A. J. Holder, T. I. Hyde and M. Schröder, *J. Chem. Soc., Chem. Commun.*, 1989, 1433.
16 D. F. Shriver, P. W. Atkins and C. H. Langford, *Inorganic Chemistry*, Oxford University Press, 1990.
17 W. W. Brandt, F. P. Dwyer and E. C. Gyarfas, *Chem. Rev.*, 1954, **54**, 959; N. E. Tokel-Takvoryan, R. E. Hemmingway and A. J. Bard, *J. Am. Chem. Soc.*, 1973, **95**, 6582; E. Janes, T. Turner and L. R. Faulkner, *J. Electroanal. Chem. Interfacial Electrochem.*, 1984, **179**, 53; T. Matsumura-Inoue and T. Tominagu-Morimoto, *J. Electroanal. Chem. Interfacial Electrochem.*, 1978, **93**, 127.
18 F. P. Dwyer and E. C. Gyarfas, *J. Am. Chem. Soc.*, 1954, **76**, 6320.
19 F. Opekar and P. Beran, *Electrochim. Acta*, 1977, **2**, 249.
20 A. J. Blake, A. J. Holder, T. I. Hyde, H.-J. Küppers, M. Schröder, S. Stötzel and K. Wieghardt, *J. Chem. Soc., Chem. Commun.*, 1989, 1600.
21 S. G. Murray and F. R. Hartley, *Chem. Rev.*, 1981, **81**, 365.
22 A. G. Orpen and N. G. Connelly, *J. Chem. Soc., Chem. Commun.*, 1985, 1310; *Organometallics*, 1990, **9**, 1206.
23 R. M. Christie, Ph.D. Thesis, University of Edinburgh, 1989.
24 A. J. Blake, R. M. Christie, Y. V. Roberts, M. J. Sullivan, M. Schröder and L. J. Yellowlees, *J. Chem. Soc., Chem. Commun.*, 1992, 848.

25 B. R. James, D. Dolphin, T. W. Leung, F. W. B. Einstein and A. C. Willis, *Can. J. Chem.*, 1984, **62**, 1238; B. R. James, S. R. Mikkelsen, T. W. Leung, G. M. Williams and R. Wong, *Inorg. Chim. Acta*, 1984, **85**, 1556; N. Farrell, D. Dolphin and B. R. James, *J. Am. Chem. Soc.*, 1978, **100**, 324; F. R. Hopf and D. G. Whitten, *J. Am. Chem. Soc.*, 1976, **98**, 7422.
26 W. A. Kiel, R. G. Ball and W. A. G. Graham, *J. Organomet. Chem.*, 1990, **383**, 481 and refs. therein.
27 N. Walker and D. Stuart, DIFABS, program for empirical absorption corrections, *Acta Crystallogr., Sect. A*, 1983, **39**, 158.
28 G. M. Sheldrick, SHELX 76, program for crystal structure refinement, University of Cambridge, 1976.
29 D. T. Cromer and J. B. Mann, *Acta Crystallogr., Sect. A*, 1968, **24**, 321.
30 R. O. Gould and P. Taylor, CALC, program for molecular geometry calculations, University of Edinburgh, 1985.
31 P. D. Mallinson and K. W. Muir, ORTEP II, interactive version, *J. Appl. Crystallogr.*, 1985, **18**, 51.

Received 5th May 1992; *Paper* 2/02322I